RSC Advances

This is an *Accepted Manuscript*, which has been through the Royal Society of Chemistry peer review process and has been accepted for publication.

Accepted Manuscripts are published online shortly after acceptance, before technical editing, formatting and proof reading. Using this free service, authors can make their results available to the community, in citable form, before we publish the edited article. This *Accepted Manuscript* will be replaced by the edited, formatted and paginated article as soon as this is available.

You can find more information about *Accepted Manuscripts* in the Information for Authors.

Please note that technical editing may introduce minor changes to the text and/or graphics, which may alter content. The journal's standard Terms & Conditions and the Ethical guidelines still apply. In no event shall the Royal Society of Chemistry be held responsible for any errors or omissions in this *Accepted Manuscript* or any consequences arising from the use of any information it contains.

ROYAL SOCIETY OF CHEMISTRY

www.rsc.org/advances

Surfactant Induced Aggregation-Disaggregation of Photodynamic Active Chlorin e6 and its relevant Interaction with DNA Alkylating Quinone in Biomimic Micellar Microenvironment

Manojkumar Jadhao[†], *Piyush Ahirkar*[†], *Himank Kumar*[†], *Ritika Joshi, Oinam Romesh Meitei and Sujit Kumar Ghosh*[*]

Department of Chemistry, Visvesvaraya National Institute of Technology, Nagpur, Maharashtra, 440010, India

[†]*All the three authors have equal contribution in this article*

TOC Entry:

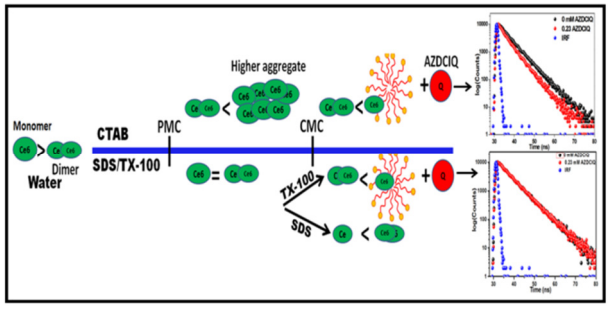

PDT active Ce6 undergoes enormous aggregation in the premicellar concentration of different surfactant systems which further disaggregated into subsequent monomer/dimer after cmc and it shows excellent dynamic interaction with alkylating quinone under study.

RSC Advances Accepted Manuscript

Abstract

The present paper epitomizes the detail physicochemical behaviour of photodynamic active chlorin e6 (Ce6) and its interaction with DNA alkylating quinone; 2,5-dichloro diaziridinyl-1,4-benzoquinone (AZDCIQ) in different bio-mimicking micellar microenvironments using steady state absorption, fluorescence, time resolved fluorescence and fluorescence anisotropy studies. The dramatic modulation in the photophysics of Ce6 has been observed in two types of surfactant assemblies namely premicellar and postmicellar assemblies of cationic CTAB, anionic SDS and nonionic TX-100. In water at pH 7.4, Ce6 exists as monomeric (73%, 4.91 ns) and dimeric (27%, 2.49 ns) forms, but with increasing concentration of CTAB in the premicellar region, the absorption and emission intensity decreases significantly due to the formation of surfactant induced higher aggregates. Interestingly further addition of CTAB (at critical micellar concentration and above) leads to disaggregation of those higher aggregates into its subsequent monomeric and dimeric form. In case of TX-100 and SDS, the dye does not form higher aggregates in premicellar region, rather it remain as monomeric-dimeric forms throughout the concentration range till critical micellar concentration (CMC). After micellization, the percentage of Ce6 monomer increases in case of TX-100, whereas the reverse case is observed in SDS, which may be explained by the forced dimerisation caused by repulsive interaction between anionic Ce6 and SDS micelles. The copper induced fluorescence quenching, solvation dynamics, and fluorescence anisotropy shows that the dye is localised in the Stern layer of CTAB, in Palisade layer of TX-100 and in outer Gouy Chapman layer or in aqueous bulk phase in case SDS micelles. The interaction of fully micellized PDT active Ce6 with DNA alkylating AZDCIQ is found to be more in CTAB as compared to TX-100 and water. The solvation dynamics of Ce6 in presence of quinone reveals the dynamic nature of the interaction

RSC Advances Accepted Manuscript

between these two partners. The spectroscopic research described herein may provide numerous effective information for the use of Chlorin(s) and alkylating quinones together to overcome the limitation of PDT, especially in hypoxic environment of solid tumor.

Keywords: Micelles, Microenvironment, Alkylating quinone, Fluorescence, Photosensitizer, Solvation dynamics, Photodynamic therapy.

Introduction:

Photodynamic therapy (PDT) has opened up new doors for the treatment of cancer with fewer side effects as compared to any other cancer treatment process. Photodynamic therapy is usually considered as a type of photochemotherapy, which requires red laser light, a photosensitizing agent, and molecular oxygen.[1–3] Typically when a photosensitizer is excited by red laser normally it returns to the ground state via triplet excited state by releasing its triplet energy. This triplet energy is concomitantly absorbed by triplet oxygen and converts itself into singlet oxygen which eventually kills the tumor cells.[4] Production of singlet oxygen is generally referred as pathway II and this is the most important process of PDT as it directly involves killing of tumour cells. On the contrary in Type I mechanism, the triplet photosensitizer reacts with the substrate and form free radicals such as peroxide radical which leads to cytotoxic events in PDT[2], especially in hypoxic environments. Solid tumor are often hypoxic in nature, hence the direct killing of tumour cell by type II mechanism is limited due to hypoxia.[5] To overcome the limitation of solid tumor due to hypoxia Alegria et al.[1] has used other molecule whose redox potential is nearly equal or more positive than oxygen. According to this hypothesis, since red-light-absorbing dyes photoreduce oxygen, these should also photoreduce molecules having nearly equal or more positive redox potentials than oxygen in anoxic/hypoxic

RSC Advances Accepted Manuscript

cells and if this reducible substrate is a DNA alkylating quinone which is activated by reduction and ultimately result in DNA alkylation with consequent cell death.[6–8] To support the above hypothesis, complete understanding of the physicochemical behaviour of PDT dyes in absence and presence of alkylating quinone in the cellular environment is necessary. In this context Ce6 has been used as a probe in this present article along with the DNA alkylating quinone in different bio-mimicking micellar systems. Ce6 is a derivative of chlorophyll and has improved its efficiency as compared to first generation photosensitizer from hematoporphyrin derivatives.[9] The therapeutic efficacy of the macrocycle Ce6 may depend on its aggregation, aggregation-disaggregation behaviour, localisation and interaction pattern (in absence /presence of alkylating quinone) in the cellular environment.

Different micellar systems have been used to monitor the bioactive probe molecules because of its cell like structure and hence micelles are often used as membrane bio-mimicking agent.[10–12] The importance of membrane in biological systems lies in their capacity to provide a matrix for arranging the reaction sequentially for efficient interaction. Substrate molecules may be sequestered and organized in the micellar interior or on the micellar boundary.[13,14] The penetration of PDT probe in micellar media may modify its photophysical behaviour because micelle produces nonpolar-polar interfaces where absorption, emission properties of dyes becomes enhanced or quenched.[15,16] The encapsulation of this PDT dye and the DNA alkylating quinone in single organized assembly can bring them together, which may result in increased possibility of the association between these two or it may alter their interaction pattern.[17] Charges on micelle may also influence pronounced effect on such types of interactions.[17] Ce6 is a well-known highly effective PDT dye[18–20] and several studies have been investigated using it as probe[21–23] but to the best of our knowledge the interaction of this PDT active Ce6 and DNA

RSC Advances Accepted Manuscript

alkylating quinone in bio-mimicking micellar microenvironment system has not been reported so far. In the present article, a conspicuous attempt has been made at first to demonstrate the physicochemical studies of Ce6 in different micelles i.e. cationic (CTAB), neutral (TX-100), anionic (SDS) and then to monitor the interaction of Ce6 with DNA alkylating quinone 2,5-diclorodiaziridinyl-1,4-benzoquinone (AZDCIQ) in aqueous as well as in above three micellar microenvironment using UV-Visible absorbance, steady state fluorescence, fluorescence anisotropy and time resolved fluorescence study to epitomize the nature and strength of interaction between PDT dye Ce6 and alkylating quinone AZDCIQ inside cell like environment. This may be a relevant addition to use PDT dyes and reducible substrate together in anoxic/hypoxic environments and it may open up new avenues for PDT treatment.

Result and Discussion:

Physicochemical properties of Chlorin e6 in a different micellar microenvironment:

The absorption and fluorescence techniques are widely used to characterize the micellar organization because of their non-invasive and intrinsic sensitivity.[24] Therefore, the changes in absorption and emission spectrum of Ce6 have been monitored in order to decode the characterization of this PDT dye in bio-mimicking micellar microenvironment of nonionic TX-100, cationic CTAB and anionic SDS.

In aqueous solution at pH 7.4, Ce6 shows two distinct absorbance bands at 401 nm (Soret band) and 653 nm (Q band). The Soret band (B) arises due to $\pi \rightarrow \pi^*$ transition and is most common in porphyrin compounds, whereas Q band is a lower energy band and its position sensitive to the chemical structure and to the changes in the microenvironment around the

RSC Advances Accepted Manuscript

porphyrin or Chlorin ring.[25] The absorption spectrum of Ce6 shows spectral variation with increasing concentration of TX-100, CTAB and SDS separately throughout the tested concentration range (Figure 1). In postmicellar concentration, B band exhibit a shift from 401 nm to 405 nm in all three micelles while Q band shows 10 nm (653 to 663 nm) and 11 nm (653 to 664 nm) red shifts for TX-100 and CTAB respectively. This bathochromic shift in the Q band of Ce6 in CTAB and TX-100 suggest that the ground state of Ce6 is somehow destabilised and reflects a lowering in the polarity of the micellar solution as compared to the aqueous medium.[26,27] In postmicellar concentration of SDS, Q band is blue shifted from 653 nm (in water at pH 7.4) to 640 nm with a hump at 668 nm. This could probably because of the formation Ce6 dimer in that particular environment (detailed discussed later on).

Surfactant induced aggregation –disaggregation of Ce6:

The emission spectra of Ce6 in aqueous solution at pH 7.4 consist of a single band at 655 nm. In premicellar concentration of non-ionic TX-100 (0 to 0.20 mM), emission spectra of Ce6 has shown a little blue shift (4 nm) with decrease in intensity. On further increase in the TX-100 concentration (0.25 to 1.1 mM), fluorescence properties of Ce6 have changed significantly as shown in Figure 2a. Here, the emission maximum also exhibits 11 nm red shift (from 655 to 666 nm) with a considerable enhancement in the fluorescence intensity. The position and intensity variation in emission spectrum can be rationalised to the change of polarity in the microenvironment due to micellization of the probe molecule or due to binding of the same with surfactant self-assemblies. In this regard, the changes in the photophysical properties of Ce6 have been studied in different dioxane-water mixtures and it reflects similar observation (discussed in next section). For better understanding, time resolved fluorescence measurement of

RSC Advances Accepted Manuscript

Ce6 in aqueous as well as in micellar environment of TX-100 has also been performed. In water (pH 7.4), the Ce6 exists as monomer (4.91 ns, 73%) and dimer (2.49 ns, 27%), whereas in the pre-micellar concentration of non-ionic TX-100 (0.02 to 0. 20 mM), the percentage of monomer (4.54 ns) and dimer (2.44 ns) rehabilitated to 55% and 45% respectively (Table 1). Hence, life time measurement indicates the premicellar dimerization of Ce6 in TX-100 which is subsequently disaggregates into its monomeric form (6.20 ns, 73.0%) at critical micellar concentration (CMC) and above.

As described earlier, in TX-100, the probe molecule altered the spectral position as well as intensity only after CMC, but in cationic CTAB, it started unusual spectral exhibition at the very low concentration of the surfactant monomer (Figure 2b). In presence of 0.001 mM of CTAB, Ce6 displays a distinct premicellar aggregation until 0.09 mM of surfactant concentration (Figure 2b). The dramatic decrease in the emission intensity of Ce6 in concentration range of 0 to 0.09 mM (Figure S1) may be explained by the interaction of the anionic probe molecule with cationic surfactant monomer, which actually forces the probe molecules to aggregate till premicellar concentration of 0.09 mM. This phenomenon has further got its confirmation from the lifetime measurement of the dye in presence of respective CTAB concentration (Table 1). Moreover the observed 11-11.5 nm bathochromic shift (655-666.5 nm) in the emission spectra at around 0.02 mM of CTAB (much below its CMC) is similar to that observed in postmicellar concentration of TX-100 and interestingly after 0.02 mM CTAB concentration the emission maxima remain unchanged even after CMC. This shift in the emission spectra in the premicellar region of CTAB may be attributed to the change in polarity around the probe. In CTAB, electrostatic attraction between the anionic dye and cationic surfactant molecule plays an important role. Ce6 molecules are attracted in the vicinity of the surfactant molecule and interact with the polar positively

RSC Advances Accepted Manuscript

charged head group of cationic surfactant. This also increases the chances of the self-aggregation of the probe molecule (confirmed later on by time resolved measurement). In addition to this, the electrostatic attraction may influence the polarity around the probe significantly in CTAB as compared to the non-ionic TX-100, where the same is not the operative mechanism. Thus in fully micellized CTAB, the probe molecules may be present in the less polar region of the cationic CTAB micelle.

In time resolved measurement, the dye shows the existence of its monomer, dimer as well as higher aggregates in CTAB solution. On addition of CTAB (0 to 0.01 mM), the percentage of monomer (higher lifetime species) decreases from 73% to 53% whereas the percentage of dimer (lower lifetime species) increases from 27% to 47% (Table 1). However in the concentration range of 0.022 to 0.09 mM of CTAB, the probe molecule exhibit best fit tri-exponential decay with three species having fluorescence lifetime 90 ps (±12 ps), 2.68 ns and 5.7 ns. It is pertinent to mentioned here that the ability to measure short lifetimes is generally determined by the excitation pulse width and the temporal response of the detector. The error percentage in the measured shortest lifetime 90 ps (±12 ps) is in little higher side due to the limitation of our experimental setup but it is till acceptable as it has obtained from the best tri-exponential fitting with lowest residuals (Figure S2) and minimum χ^2 (chi-square statistic) value as compared to the single and bi-exponential fitting, which reflect much larger residuals and higher χ^2 values. The shortest lifetime may be due to the formation of higher aggregates[28,29] along with existing monomeric and dimeric species. Further addition of CTAB leads to the disaggregation of higher aggregates into its subsequent monomeric and dimeric form as reflected in the lifetime measurement (Table 1) and after CMC (1 mM), Ce6 remains mostly as monomer (75%) in

RSC Advances Accepted Manuscript

CTAB micelle. This observation is in line with the increase in emission intensity of Ce6 in fully micellized CTAB concentration. (Figure S1).

In premicellar region of SDS micelle, Ce6 has shown single emission peak at 655 nm (Figure 2c) and thereafter in postmicellar region it exhibits hypsochromism (644 nm) with a small shoulder at 666 nm but the emission intensity remains invariant after CMC. This observation can be explained on the basis of force aggregation of Ce6 induced by likely charged SDS micelle. In premicellar region, the negatively charge SDS molecule remains in monomeric or in smaller aggregated form[30–32] and therefore interacted to a lesser extent with negatively charged Ce6 molecule. At this concentration region, the repulsion between likely charged micelle and Ce6 is much lesser. On further increase in the concentration of surfactant, the size of surfactant aggregate grows and at CMC when it finally forms the negatively charged micelle, it enhances the repulsive interaction with the dye molecule. Hence, anionic micelle enforces the negatively charged Ce6 to come closer, resulting adverse dimerization in the outer Gouy-Chapman layer or in the aqueous bulk phase. This is practically manifested by the very weak interaction between Ce6 and SDS micelles. Force dimerization of Ce6 in postmicellar region of SDS has further been confirmed using life time measurement. In premicellar concentration of SDS, Ce6 exists as 56% monomer and 44% dimer, while in postmicellar concentration, the observed higher percentage of Ce6 dimer (87%) validates the above assumption of SDS micelle induced forced dimerization (Table 1).

Hence the above photophysical studies of Ce6 in aqueous, nonionic TX-100, cationic CTAB and anionic SDS micellar environments, reflects that the Ce6 dye interacting strongly with CTAB and TX-100 micelle whereas very less interaction occurs in case of SDS. In CTAB, higher aggregates of Ce6 are observed in premicellar region which subsequently disaggregate

RSC Advances Accepted Manuscript

into Ce6 monomer near CMC and above. In case of TX-100 the dimer percentage increases in the premicellar region, and reverse case is observed with increasing percentage of monomer along with the red shift in emission maxima in postmicellar case. In SDS, the force dimerization of Ce6 (with 11 nm blue shift in emission maxima) is observed in postmicellar region of SDS micelle. The red shift in the emission spectra of Ce6 in TX-100 and CTAB micelle suggests the decrease in polarity around the Ce6 molecules. Hence, Ce6 molecules may be trapped inside the less polar environment of these micelles, where as in SDS the dye probably resides in the outer Gouy-Chapman layer or in the aqueous bulk phase.

Table 1: Fluorescence lifetimes with fraction of emitting species of Ce6 in Water, CTAB, TX-100 and SDS micellar media at 298 K.

Ce6 in	**τ_1 (ns)**	**α_1 (%)**	**τ_2 (ns)**	**α_2 (%)**	**τ_3 (ns)**	**α_3 (%)**	**χ^2**
Water	4.91	73.0	2.49	27.0			1.31
CTAB							
0.001 mM	5.11	53.0	3.09	47.0			1.37
0.02 mM	5.70	9.0	2.68	9.0	0.09 (±0.012)	82.0	1.57
0.09 mM	4.65	4.0	1.39	10	0.08 (±0.015)	86.0	0.89
0.50 mM	3.91	28.0	0.75	72.0			1.33
1.0 mM	5.61	71.0	2.22	29.0			1.49
2.0 mM	5.66	75.0	2.29	25.0			1.35
TX-100							
0.02 mM	4.13	57.0	2.54	43.0			1.03

RSC Advances Accepted Manuscript

0. 2 mM	4.54	55.0	2.44	45.0	1.07
2.0 mM	6.20	73.0	3.59	27.0	1.30
SDS					
3.0 mM	4.58	56.0	2.50	44.0	1.10
6.0 mM	4.75	49.0	2.71	51.0	1.14
14.0 mM	4.82	13.0	3.13	87.0	1.07

Polarity sensitive spectral behaviour of Ce6:

The comparison of spectral properties of a fluorophore in biomimicking systems such as micelle, reverse micelle, proteins and lipids with those in solvents of known polarity can reveal the micropolarity in vicinity of the fluorophore.[33] The empirical solvent polarity parameter $E_T(30)$ provides a quantitative approach for the determination of micropolarity surrounding the probe molecule in biphasic environment,[34,35] and a graded series of dioxane-water mixture against $E_T(30)$ has been widely used for this purpose.[36,37] Considering these facts, the absorption (Figure S3) and emission spectra of Ce6 (Figure 3) have been recorded in various dioxane-water mixtures of known $E_T(30)$ values.[36] As discuss earlier, absorption spectrum of Ce6 in an aqueous solution (pH 7.4) shows two distinct bands at 401 nm (B band) and 653 nm (Q band). In the present experiment the B band shows a very small change in its position on increasing the dioxane percentage (decreasing polarity) in the solvent mixture hence no attempt has been made to analyse these data. On the other hand, Q band has reflected more sensitivity towards the change in micropolarity surround the probe. A 5 nm negative solvatochromism in the Q band absorption is evident upon addition of 5% dioxane to the system. However on gradual addition of

RSC Advances Accepted Manuscript

dioxane to about 70%, a continuous red shift of 10 nm is noticed and thereafter the band position does not change till 90% of the dioxane content (Table 2). The emission maxima of Ce6 have shown the similar trend, where it is initially 2 nm blue shifted in addition of 5% of dioxane in water. On successive increase in dioxane content (until 70%), 11 nm red shift is observed and afterwards it remain constant (Figure 3). The drift in the absorption and emission maxima of Ce6 in the solvent mixture exist till 70:30 dioxane: water ratio (E_T (30) = 50.5 kcal mol^{-1}) and afterwards both the maxima become levelled off at 663 nm and 666 nm respectively (Table 2). This indicates that the photophysical properties of Ce6 are highly polarity sensitive in nature. Similar photophysical changes have also been observed during the interaction of Ce6 with nonpolar TX-100 micelle as discussed in earlier section. Hence, this simple but informative experiment suggests that the micropolarity around the Ce6 probe in TX-100 micelle resembles with 70:30 dioxane: water mixture and it may be predicted that the probe is present in the less polar region of TX-100 micelle that probably corresponds to the range of E_T (30) value 50.5-46.6 kcal mol^{-1}.

Table 2: Photophysical data of Ce6 in Dioxane-water mixtures, λ_{abs} (nm), λ_{em} (nm) and E_T (30) values[36]

Percentage of Dioxane: Water	E_T(30) value kcal mol^{-1}	λ_{abs} (nm)	λ_{em} (nm)
0:100	63.1	653	655
05:95	62.3	648	653
10:90	60.9	655	658
20:80	58.2	657	659

RSC Advances Accepted Manuscript

30:70	57.2	659	661
40:60	55.8	660	663
50:50	53.2	661	664
60:40	52.0	662	665
70:30	50.5	663	666
80:20	48.7	663	666
90:10	46.6	663	666
100:0	36.3	664	667

Location of Chlorine e6 in micellar microenvironment:

Identification of rotational confinement of Ce6 in micellar microenvironment:

Steady state fluorescence anisotropy study has always occupied a position of central importance because of its tremendous ability to provide valuable information about the microenvironments in the immediate vicinity of the fluorophore.[38] It is a sensitive indicator of average angular displacement of fluorophore that occurs between absorption and subsequent emission of photon.[39] Hence, it helps to examine the physical characteristics and the degree of rigidity imposed by confined micellar media on the microenvironment of the fluorophore as compared with unrestricted surrounding in aqueous solution. Thus, fluorescence anisotropy study of Ce6 has been monitored to get better insight about the change in rotational restriction in micellar environments. In aqueous solution, the anisotropy value (r) of Ce6 is found to be 0.06. A little high r value in an aqueous medium (at pH 7.4) may be explained by the existence of the

RSC Advances Accepted Manuscript

monomer (73%) and dimer (27%) forms of Ce6. In aqueous medium, fraction of Ce6 molecules remains in dimer form. The dimerization causes the rotational restriction as compared to the free monomer and enhances r value. In case of TX-100 and CTAB, r value of Ce6 increases with increase of concentration and when all the molecule are fully micellized, it reaches to a constant value.[40,41] The constant r value in TX 100 and CTAB micelle is found to be 0.20 and 0.12 respectively (Figure 4). The anisotropy values of Ce6 in TX-100 and CTAB micelle strongly indicates the fluorophore is located in more confined environment i.e. inside the micelle rather than outer bulk phase. The relative variation in the r values suggest that the probe is located deeper inside in TX-100 medium than that in CTAB. This observation supports the following phenomenon. In cationic micelle, both hydrophobic and electrostatic interaction comes into play for negatively charge fluorophore and therefore Ce6 orient itself towards the Stern layer rather towards nonpolar core. However, in nonionic micelle only hydrophobic forces are active, and thus, Ce6 may reside in the low polarity region of the nonionic micelle. Thus the above result suggests that the Ce6 probe is buried deep in TX-100 compared to CTAB micelle. However, in case of SDS we are unable to measure the rotational confinement because of weaker or almost no interaction of the fluorophore with SDS micelles. It is pertinent to mention here that in both CTAB and TX-100, in premicellar region, the dye Ce6 undergoes a enormous aggregation, which may have a profound effect on its anisotropy value, but the stated aggregation leads to a massive decrement of emission intensity and hence it becomes unmanageable to measure the anisotropy value (r) with acceptable error limit in the premicellar concentration range. However beyond this concentration, the dye disaggregates into its monomeric form and hence emission intensity gradually increases, which provides a fair chance to measure its anisotropy value that perhaps predominantly comes from the confined monomer in the respective surfactant solution.

RSC Advances Accepted Manuscript

Fluorescence quenching of Ce6 by metal ion:

The fluorescence quenching experiment has been employed to determine the location of the probe in the three competing regions i.e. aqueous bulk phase, interfacial region and deeper nonpolar core region of the micelles. In fluorescence quenching, the availability of quencher to the fluorophore is necessary as both, static and dynamic quenching requires molecular contact between the two interacting partner.[39] Thus, the fluorescence quenching experiment of Ce6 in fully micellized condition of all three surfactant has been performed by using Cu^{2+} ion as a quencher. The idea behind using Cu^{2+} is that the ionic quencher ion is available in aqueous phase as well as in the micelle-water interface [42] but not to the micellar core due to very low polarity in the said region.[27] Moreover, the emission from the solution in a fluorescence quenching experiment containing Ce6 and Cu^{2+} comes exclusively from the micelle containing excited probe i.e. from the "photo selected" population.[43,44] The quenching efficiency of Ce6 by Cu^{2+} in all three different micelle is quantified by well-known Stern-Volmer equation:

$$\frac{F_0}{F} = 1 + K_{sv}[Q] \quad (1)$$

Where, F_0 and F are the fluorescence intensity of dye in absence and presence of quencher and K_{sv} is Stern-Volmer constant. [Q] is the concentration of Cu^{2+}. The bimolecular quenching rate constant (k_q) for the above reaction has been calculated using the relation $K_{sv} = k_q\tau$, where τ is the average lifetime of dye in respective micellar solution. The obtained K_{sv} and k_q values in nonionic and ionic micelles follows the order SDS > TX-100 > CTAB (Table 3). The higher values of K_{sv} in 10^{6-4} order and the estimated k_q value at 298 K in the order of 10^{13-14} is much greater than the maximum possible value of the diffusion controlled quenching (i.e., 2.0 x 10^{10} L mol^{-1} s^{-1}).[45,46] Hence it may be assumed that the interaction between the cationic quencher Cu^{2+} and the negatively charge Ce6 in all these three micelles is static in nature. The

RSC Advances Accepted Manuscript

Cu^{2+} ion has decreased the emission intensity of the probe molecule more efficiently in SDS micelle as compared to the CTAB and TX-100 (Figure 5). This observation may be rationalised by the fact that in SDS micelle the anionic probe is likely to be present in the outer Gouy-Chapman layer or in the aqueous bulk phase (as discussed in earlier section) and herby easily accessible to the cationic quencher ion Cu^{2+}, whereas in nonionic TX-100, dye is perhaps located in the less polar region of the surfactant self-assembly and is moderately available to the Cu^{2+} ion resulting lesser quenching efficiency than SDS. This explanation is also in line with the result that obtained in fluorescence anisotropy and polarity sensitive experiment as discussed earlier. On contrary, the insignificant quenching that has observed in case CTAB, gives an indication of electrostatic repulsion between likely charged quencher ion and the cationic micelle that reduces the chances of interaction between them, thus, the quenching process becomes unfavourable. Hence the metal ion (Cu^{2+}) quenching experiment suggests that the PDT active dye Ce6 is localised in the outer Gouy-Chapman layer or in aqueous bulk phase in case SDS micelle, in the less polar palisade layer of TX-100 and in Stern layer of CTAB micelle predominantly.

Table 3: Values of Stern-Volmer constant (K_{sv}) and bimolecular rate constant (k_q) in different micelle.

Surfactant	K_{sv} (lit mol^{-1})	k_q (lit mol^{-1} s^{-1})
SDS (14 mM)	1.11×10^6	3.32×10^{14}
TX-100 (2 mM)	2.47×10^5	4.49×10^{13}
CTAB (5 mM)	6.39×10^4	1.44×10^{13}

RSC Advances Accepted Manuscript

Solvation dynamics of Ce6 in different environment:

Fluorescence lifetime measurement serves as sensitive indicator of local environment around the fluorophore and it is responsive towards the excited state interaction.[47] Differential solvent relaxation around the fluorophore and/or partitioning of the fluorophore in distinct region of a confined environment give rise to differences in the lifetime of the fluorophore.[48] Lifetime measurement of Ce6 in multi component system like micelle may provide enormous information regarding location of Ce6. So the change in the lifetime of probe in microheterogeneous environment compared to water has been studied using time resolved fluorescence measurement. In time resolved fluorescence measurement Ce6 shows biexponential decay in aqueous as well as in all three different micelle under study (Figure 6). The two different lifetimes of Ce6 are attributed to two species, one is the monomer and another is dimer. The higher lifetime component probably corresponds to the monomer and lower lifetime credited to the dimer of Ce6. The preceding statement has been verified further by the time resolved fluorescence analysis of Ce6 in nonpolar solvent like cyclohexane, where the dye is expected to be present as monomeric species only, and in the stated experiment it shows 92% of the species having lifetime of 5.34 ns and rest 8% is of 1.49 ns. The later species (1.49 ns) could be the dimer that is formed as we have used a small aliquot (0.25%) of the ethanolic stock solution of Ce6 because of its insoluble nature in cyclohexane.

The average lifetime of the probe molecule in aqueous as well as in these three micellar medium follows the order TX-100>CTAB>Water (pH7.4)>SDS. The lifetime values of Ce6 in water as well as in fully micellar solution are shown in Table 4. The lifetime of Ce6 is shortened in polar aqueous medium could be because of more perturbation in its electronic state caused by the increase in energy transfer due to high dipole moment of surrounding molecule that present

RSC Advances Accepted Manuscript

in the cybotactic region. Enhanced average lifetime in case of TX-100 provides logical justification about the location of Ce6 in relatively less polar region than the aqueous solution. In CTAB, the average lifetime of probe is in between the water and TX-100, implies Ce6 remains in the comparatively more polar region than the TX-100 but less polar than the aqueous medium. In case of SDS micelle the average lifetime is found to be shorter than that of aqueous medium, when monitored at 644 nm. The least average fluorescence lifetime of negatively charged Ce6 in anionic SDS may be explained by the forced dimerization (87%) that occurs in the postmicellar region.

Table 4: Fluorescence decay parameters of Ce6 in water and micellar medium at 298 K

Environment	τ_1 (ns)	α_1 (%)	τ_2 (ns)	α_2 (%)	τ_{avg}	χ^2
Water (pH 7.4)	4.91	73.0	2.49	27.0	4.25	1.31
SDS (14.0 mM, 644 nm)	4.82	13.0	3.13	87.0	3.34	1.07
TX-100 (2.0mM, 666 nm)	6.20	73.0	3.59	27.0	5.49	1.30
CTAB (2.0 mM, 666 nm)	5.66	75.0	2.29	25.0	4.81	1.35

Hence, steady-state absorption, fluorescence anisotropy, control fluorescence quenching, and time resolved fluorescence studies demonstrate the stronger interaction of Ce6 with the nonionic TX-100 and cationic CTAB than that of anionic SDS micelle. In TX-100 and CTAB Ce6 displays a dramatic modulation in the photophysical properties which corresponds to variation in micropolarity around the probe and the aggregation- disaggregation behaviour of the probe molecule. In water at pH 7.4, Ce6 exists as monomeric (73%, 4.91 ns) and dimeric (27%, 2.49 ns) forms, but with increasing concentration of CTAB in the premicellar region surfactant

RSC Advances Accepted Manuscript

induced higher aggregates formed. Interestingly further addition of CTAB leads to disaggregation of those higher aggregates into its subsequent monomeric and dimeric form. In case of TX-100 and SDS, the dye does not form higher aggregates in premicellar region, rather it remain as monomeric-dimeric forms throughout the concentration range till CMC. After micellization, the percentage of Ce6 monomer increases in case of TX-100, whereas the reverse case is observed in SDS, which is explained by the forced dimerisation caused by repulsive interaction between anionic Ce6 and SDS micelles. In control fluorescence quenching experiment, Stern Volmer quenching constant K_{sv} and bimolecular rate constant k_q value follow the order SDS>TX-100>CTAB, which indicates that the probe molecule is trapped in the less polar environment of both TX-100 and CTAB as compared to SDS and it is not easily available for the cationic quencher to collide. The least k_q value in CTAB elucidates the repulsion between the likely charge quencher and the Stern layer of the cationic micelle. However the fluorescence anisotropy and lifetime measurement implies that the Ce6 is located deeper inside in the TX-100 micelle as compared to CTAB. Thus, by correlating all the above three experiments we can conclude that the Ce6 probe is located in a less polar palisade layer of TX-100 and held at the positively charged Stern layer by the favourable electrostatic interaction in CTAB micelle. In case of SDS micelle, fraction of the Ce6 molecules remains in the outer Gouy-Chapman layer or in the aqueous bulk phase.

Interaction of DNA alkylating quinone (AZDCIQ) with Chlorin e6 in aqueous and different surfactant systems:

Interaction between Ce6 and AZDCIQ has been studied in aqueous as well as fully micellized CTAB and TX-100 medium under anaerobic condition at pH 7.4 using UV-Vis

RSC Advances Accepted Manuscript

absorption, steady state emission and time resolved fluorescence spectroscopy. The absorption and emission spectra of dye has been recorded with gradual addition of AZDCIQ in aqueous and different micellar solution. The extent of interaction between AZDCIQ and the PDT active Ce6 has been estimated by calculating the association constant of AZDCIQ in the above mentioned systems using following equation:

$$\log\left(\frac{F_0-F}{F}\right) = \log(K_a) + n\log[AZDCIQ] \quad (2)$$

Where F_0 and F are the fluorescence emission intensity in absence and presence of AZDCIQ, [Q] is concentration of AZDCIQ and K_a is association constant between the dye and the quinone molecule. The association constant in aqueous, CTAB and TX-100 is found to be 1.2 x 10^3 M^{-1}, 1.9 x 10^3 M^{-1}, and 1.3 x 10^1 M^{-1} respectively (Figure 7). The variation in K_a values of alkylating quinone with Ce6 in the different micellar media is due to diverse accessibility of probe to the quinone molecule. The diminution emission intensity of Ce6 on gradual addition of AZDCIQ in aqueous medium, TX-100 and CTAB micelle (Figure S4) point towards the interaction of this PDT active dye with the DNA alkylating quinone and the interaction is more prominent in CTAB (where the Ce6 molecules are present in the Stern layer) as compared to aqueous medium and lesser in TX-100 (where the Ce6 molecule are located in thick palisade layer of micelle). The above observation signifies that the quinone molecule interacting with the exposed Ce6 molecule i.e. the dye, which present in bulk aqueous phase or in the interfacial layer (i.e. Stern layer) rather than those present deeper inside the micelle.

In order to achieve a better understanding about the dye-quinone interaction, time resolved fluorescence experiments have also been performed. On addition of AZDCIQ in aqueous and in CTAB micellar medium the fluorescence decay profile varies such that it is

RSC Advances Accepted Manuscript

comparatively faster in CTAB than in aqueous medium (Figure 8 a and b). On the contrary, TX-100 shows no change in the fluorescence decay profile upon addition of the quinone molecule (Figure 8c). The Stern-Volmer plot of increasing concentration of AZDCIQ with (τ_0/τ) is represented in Figure 9. The variation of K_{sv} (Table 5), that is calculated from average lifetime of Ce6 gives an indication of the dynamic interaction between these two interacting partner which may be caused by the electron or energy transfer mechanism.

Thus from the steady state absorption, fluorescence and time resolved fluorescence, we may conclude that AZDCIQ interact considerably with the PDT active dye that is localised in the vicinity of the Stern layer or at the interface of the micelle as well as in the bulk solution. The higher association constant and faster fluorescence decay in CTAB micelle suggest a change in the mechanism of interaction where both the partners are brought together in the confined micellar microenvironment and thereby, increasing their chances of interaction manifold and that ultimately serves the basic purpose of this article.

Table 5: Change in average lifetime and Stern-Volmer constant of Ce6 by AZDCIQ in water, CTAB and TX-100

Environment	[AZDCIQ] (M)	Average lifetime (ns)	K_{sv} (lit/mol^{-1})
Water	0	4.37	
	2.31×10^{-4}	3.73	6.50×10^{2}
CTAB (5.0 mM)	0	4.81	
	2.31×10^{-4}	3.50	1.70×10^{3}
TX-100 (2.0 mM)	0	5.49	
	2.31×10^{-4}	5.46	

RSC Advances Accepted Manuscript

Identification of dynamic quenching behaviour by quantum chemical calculations:

To identify the exact mechanism of the above said dynamic interaction between AZDCIQ and Ce6, Density Functional Theory (DFT) and Time dependent DFT (TD-DFT) have been employed for all possible structures of dye and the quinone molecule using Gaussian 09 programme.[49] The geometries of Ce6 and AZDCIQ as neutral as well as charged species are fully optimized using B3LYP hybrid density functional with 6-31G basis set. The neutral molecules are optimized using restricted Kohn Sham equation whereas the charged species are optimized using unrestricted Kohn Sham equation.[50] The excited state calculations are achieved using TD-DFT and the same functional along with the same basis set.

The geometry of Ce6 and AZDCIQ are fully optimized in the ground state as well as their respective excited state. Ce6 cation and AZDCIQ anion are further optimized to study the electron transfer process from the former to the later one. Photoexcitation of Ce6 can lead to either an energy transfer or an electron transfer to AZDCIQ as indicated by the diminution of emission intensity experimentally. The former (energy transfer) may excite the AZDCIQ molecule while the later (electron transfer) may lead to the formation of their respective ions. The energy transfer is probably feasible if the sufficient energy for the excitation of AZDCIQ molecule can be supplied by the Ce6 dye. However, the difference between the ground state and the first singlet state of Ce6 are found to be 2.14 eV and it is insufficient for the excitation of AZDCIQ molecule which is found to be 3.34 eV that obtained from the vertical excitation using TD-DFT methodology. Thus, it may be unlikely that on photoexcitation Ce6 dye will lead to an energy transfer to the quinone molecule.

RSC Advances Accepted Manuscript

On the other hand, Ce6 and AZDCIQ are compared on the basis of the stability of their respective ions that produced, if an electron transfer reaction is taking place. The anion of the AZDCIQ molecule is found more stable as compared to the neutral molecule by 32.76 kcal/mol. This indicates that any electron transfer process leading to the formation of AZDCIQ anion is favourable. Moreover an electron transfer process accompanied by the protonation in aqueous environment may lead to the formation of dihydroquinone (DHQ) [1,8], further protonation of the DHQ may lead to the formation of open ring AZDCIQ as shown in Scheme 1. The calculated energies on the optimized geometries of DHQ and open ring show that they are more stable than the AZDCIQ anion. DHQ is highly stable as compared to the AZDCIQ anion by 729.63 kcal/mol. The huge difference in the energies indicates that the formation of DHQ is highly favourable. Further the open ring structure of AZDCIQ is much more stable than the AZDCIQ anion by 1142.27 kcal/mol and DHQ by 412.64 kcal/mol. The differences in the energy values (between the anion and the DHQ and the corresponding open ring structure) suggest that after the electron transfer, the formation of the open ring is more favourable than the formation of DHQ. Moreover the formation of open chain may be followed by the nucleophilic attack as demonstrated in Scheme 1. Hence as far as theoretical calculations are concerned, there is an indication that the PDT active dye Ce6 and the DNA alkylating quinone AZDCIQ share an electron transfer mechanism which justifies their dynamic nature of interaction. However the experimental counterpart e.g. time resolved absorption studies by laser flash photolysis will be attempted to in our future work to corroborate the same.

RSC Advances Accepted Manuscript

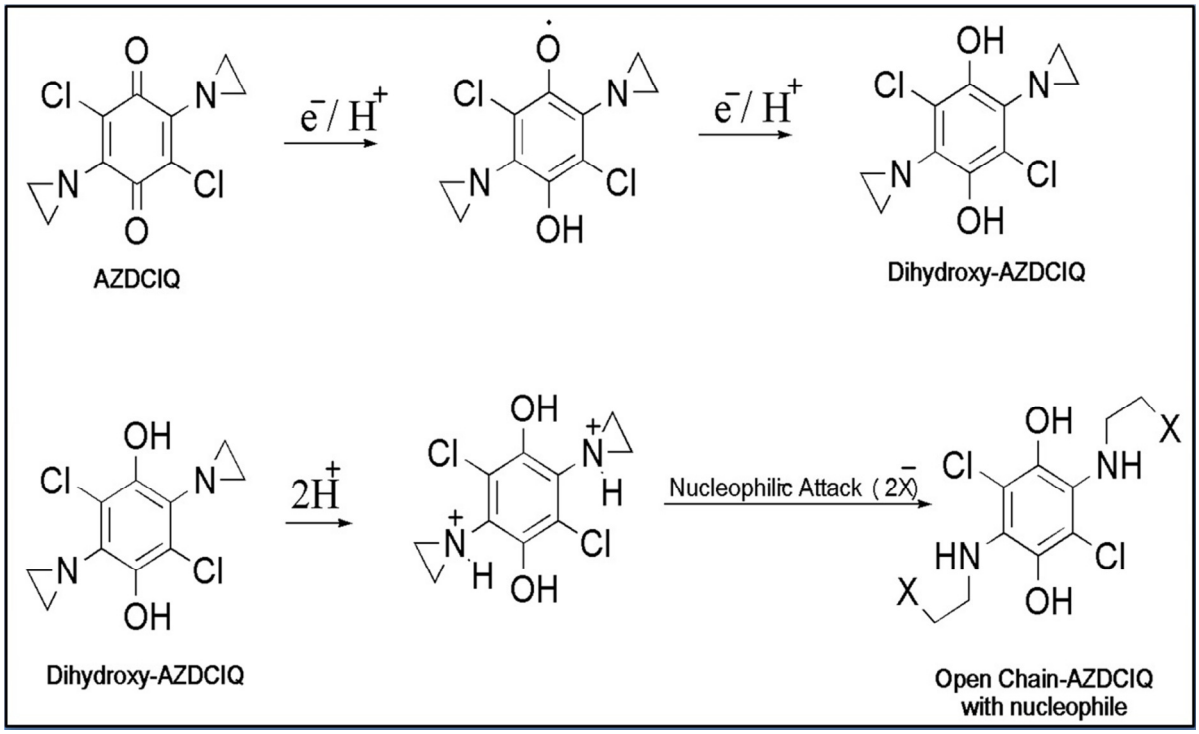

Scheme 1: Proposed electron transfer mechanism from Ce6 to AZDCIQ.

Experimental:

Materials:

The Ce6 dye was procured from Frontier Scientific, USA and used as received. The alkylating quinone 2,5-dichloro-diaziridinyl-1,4-benzoquinone (AZDClQ) and surfactant TX-100, CTAB, and SDS were obtained from Sigma Aldrich Chemicals, USA and used as received.

Instrumentation and methodology:

The steady state absorption and emission were recorded at 298 K using Jasco V-630 spectrophotometer equipped with peltier accessories and Jasco FP-8300 spectrofluorometer equipped with temperature controller unit respectively. All the measurements were carried out using 1.0 cm quartz cell and an external slit width of 2.5 nm. The steady state fluorescence

RSC Advances Accepted Manuscript

anisotropy has also performed using Jasco FP-8300 spectrofluorometer along with polarizer accessories. For the anisotropy measurement the excitation and emission bandwidths were 2.5 nm each. The steady state anisotropy is calculated by the following equation:

$$r = (I_{VV}-GI_{VH})/(I_{VV}+2GI_{VH}) \quad (3)$$

where I_{VV} and I_{VH} are the emission intensities obtained with the excitation polarizer oriented vertically and the emission polarizer oriented vertically and horizontally, respectively. The factor G is defined as I_{HV}/I_{HH}. Fluorescence lifetime measurement were performed with PTI Time Resolved Spectrofluorimeter Pico Master (PTI, HORIBA, USA) using a light emitting diode (407 nm) as a light source and time correlated single photon counting (TCSPC) technique. The pulse width of PTI light emitting diode is typically in the range of 700-1100 ps (LED dependent), while, PMD-2 detector have a response time of approx. 180 ps, temporal resolution is about 813 fs and is well designed to provide a uniform response over the entire area of the photocathode. Emission spectral range of the detector is 185-820 nm. The data has been analysed using *FelixGX* 4.1.2 decay analysis software. The exponential fittings were authenticated by reduced χ^2 criterion and the randomness of the fitted function of the raw data. The average fluorescence lifetime $<\tau>$ for biexponential decay of the dye was calculated using decay times (τ_i) and the relative contribution of components (α_i) in following equation [39].

$$<\tau>_{=}\sum\tau_i\alpha_i/\sum\alpha_i \quad (4)$$

All the above experiments were repeated in order to obtain reproducible results.

Sample preparation:

Millipore water has been used for preparing all the solutions and the pH was adjusted as required. Oxygen was excluded from samples by keeping a positive pressure of Argon during all the experiments. Deoxygenation has been stopped while recording the absorption and emission

RSC Advances Accepted Manuscript

spectra. The stock solution of Ce6 was prepared in ethanol and 2, 5-dicloro-diaziridinyl-1,4-benzoquinone (AZDClQ) stock was prepared by warming it in aqueous solution followed by cooling and filteration. The different surfactant solutions were prepared by dissolving required amounts of CTAB, SDS or TX-100 in millipore water at pH 7.4.

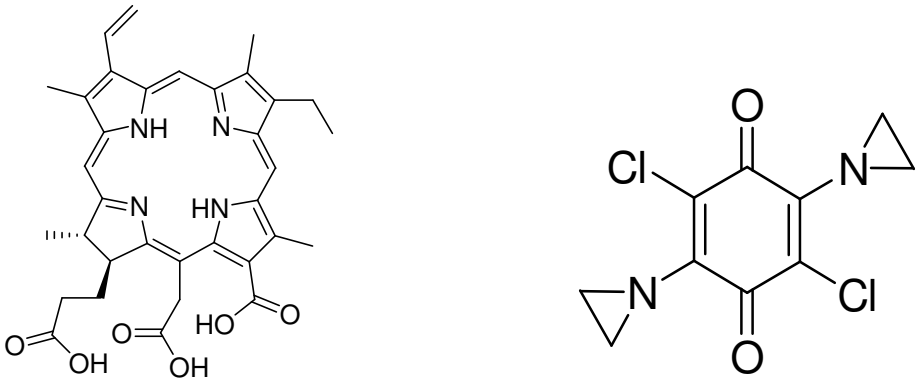

(a) (b)

Scheme 2: Structure of (a) Ce6 and (b) AZDCIQ.

Conclusion:

In brief, the present article has given emphasis on the interaction of PDT active Chlorin e6 with different biomimicking microenvironment and its consequences in terms of aggregation-disaggregation, polarity sensitive behaviour and its localisation. This could be extremely informative as the therapeutic activity of Chlorin (s) largely depends on the on its aggregation-disaggregation behaviour, localisation and interaction pattern in the cellular environment. Moreover the desired interaction of fully micellized PDT active dyes with DNA alkylating quinones and its characterisation by experimental and theoretical spectroscopic approach may also have enormous significance to identify the exact mechanism of photosensitised reduction

RSC Advances Accepted Manuscript

and subsequent DNA alkylation especially in hypoxic environment of solid tumor. The consolidated spectroscopic research described herein may warrant extended investigation of PDT dye-Quinone-DNA system in cell like environment.

Acknowledgement:

SKG gratefully acknowledge the financial support from Department of Science and Technology, India (Project no. SR/FT/LS/-172/2009). MJ gives thanks to DST for providing SRF, PA gives thanks to VNIT for providing research fellowship. Thanks to S. Power and S. Nagdeve for their kind help. SKG thanks to Dr. R. M. Patrikar, Centre for VLSI and Nanotechnology, VNIT, Nagpur for providing Gaussian suite for theoretical calculation. Authors appreciate and thanks to anonymous reviewers for their kind suggestion to improve the quality of the manuscript.

References:

1 A. E. Alegria, N. Cruz-Martinez, S. K. Ghosh, C. Garcia and R. Arce, *J. Photochem. Photobiol. A Chem.*, 2007, **185**, 206–213.

2 M. Ochsner, *J. Photochem. Photobiol. B.*, 1997, **39**, 1–18.

3 D. E. J. G. J. Dolmans, D. Fukumura and R. K. Jain, *Nat. Rev. Cancer*, 2003, **3**, 380–387.

4 M. C. DeRosa and R. J. Crutchley, *Coord. Chem. Rev.*, 2002, **233-234**, 351–371.

5 T. M. Busch, S. M. Hahn, S. M. Evans and C. J. Koch, *Cancer Res.*, 2000, **60**, 2636–2642.

RSC Advances Accepted Manuscript

6 A. E. Alegria, Y. Inostroza and A. Kumar, *Photochem. Photobiol.*, 2008, **84**, 1583–1588.

7 P. Colombo, K. Gunnarsson, M. Iatropoulos and M. Brughera, *Int. J. Oncol.*, 2001, **19**, 1021–1028.

8 R. H. Hargreaves, J. A. Hartley and J. Butler, *Front. Biosci.*, 2000, **5**, E172–E180.

9 G. A. Kostenich, I. N. Zhuravkin, A. V. Furmanchuk and E. A. Zhavrid, *J. Photochem. Photobiol. B.*, 1991, **11**, 307–318.

10 M. Haque, A. Das and S. P. Moulik, *J. Colloid Interface Sci.*, 1999, **217**, 1–7.

11 N. Sarkar, K. Das and A. Datta, *J. Phys. Chem.*, 1996, **480**, 10523–10527.

12 A. K. Dwivedi, M. Pandeeswar and T. Govindaraju, *ACS Appl. Mater. Interfaces*, 2014, **6**, 21369–79.

13 N. V Sushkin, D. Clomenil, J. Ren and G. D. J. Phillies, *Langmuir*, 1999, **15**, 3492–3498.

14 R. E. Riter, E. P. Undiks, J. R. Kimmel and N. E. Levinger, *J. Phys. Chem. B*, 1998, **102**, 7931–7938.

15 P. Banerjee, S. Pramanik, A. Sarkar and S. C. Bhattacharya, *J. Phys. Chem. B*, 2008, **112**, 7211–7219.

16 S. Mandal, V. G. Rao, C. Ghatak, R. Pramanik, S. Sarkar and N. Sarkar, *J. Phys. Chem. B*, 2011, **115**, 12108–12119.

17 T. K. Mukherjee, P. P. Mishra and A. Datta, *Chem. Phys. Lett.*, 2005, **407**, 119–123.

RSC Advances Accepted Manuscript

18 R. Bachor, C. R. Shea, R. Gillies and T. Hasan, *Proc. Natl. Acad. Sci. U. S. A.*, 1991, **88**, 1580–1584.

19 M. R. Hamblin, J. L. Miller and B. Ortel, *Photochem. Photobiol.*, 2000, **72**, 533–540.

20 A. Yuan, X. Tang, X. Qiu, K. Jiang, J. Wu and Y. Hu, *Chem. Commun.*, 2015, **51**, 3340–3342.

21 J. Wang, G. Zhu, M. You, E. Song, M. I. Shukoor, K. Zhang, M. B. Altman, Y. Chen, Z. Zhu, C. Z. Huang and W. Tan, *ACS Nano*, 2012, **6**, 5070–5077.

22 L. Banevicius, A. Genady and J. Valliant, *Soc. Nucl. Med. Annu. Meet. Abstr.*, 2013, **54**, 1179.

23 S. M. Wu, X. J. Sun, L. L. Wang, M. Y. Fei and Z. Y. Yan, *J. Nanoparticle Res.*, 2014, **16**, 2701.

24 G. B. Behera, B. K. Mishra, P. K. Behera and M. Panda, *Adv. Colloid Interface Sci.*, 1999, **82**, 1–42.

25 R. Pottier and T. G. Truscott, *Int. J. Radiat. Biol.*, 1986, **50**, 421–452.

26 P. Das, A. Chakrabarty, A. Mallick and N. Chattopadhyay, *J. Phys. Chem. B*, 2007, **111**, 11169–76.

27 A. Mahata, D. Sarkar, D. Bose, D. Ghosh, A. Girigoswami, P. Das and N. Chattopadhyay, *J. Phys. Chem. B*, 2009, **113**, 7517–26.

RSC Advances Accepted Manuscript

28 R. F. Correia, M. I. Viseu and S. M. Andrade, *Photochem. Photobiol. Sci.*, 2014, **13**, 907–916.

29 D. L. Akins and O. Serdar, 1996, **3654**, 14390–14396.

30 K. Y. Law, *Photochem. Photobiol.*, 1981, **33**, 799–806.

31 S. M. Dennison, J. Guharay and P. K. Sengupta, *Spectrochim. Acta Part A Mol. Biomol. Spectrosc.*, 1999, **55**, 903–909.

32 T. A. Fayed, *Colloids Surfaces A Physicochem. Eng. Asp.*, 2004, **236**, 171–177.

33 S. K. Ghosh and S. C. Bhattacharya, *Chem. Phys. Lipids*, 2004, **131**, 151–158.

34 S. K. Ghosh, P. K. Khatua and S. C. Bhattacharya, *J. Colloid Interface Sci.*, 2004, **279**, 523–532.

35 S. K. Ghosh, S. U. Hossain, S. Bhattacharya and S. C. Bhattacharya, *J. Photochem. Photobiol. B Biol.*, 2005, **81**, 121–128.

36 E. M. Kosower, H. Dodiuk, K. Tanizawa, M. Ottolenghi and N. Orbach, *J. Am. Chem. Soc.*, 1975, **97**, 2167–2178.

37 A. Mallick, B. Haldar, S. Maiti, S. C. Bera and N. Chattopadhyay, *J. Phys. Chem. B*, 2005, **109**, 14675–82.

38 A. Samanta, B. K. Paul and N. Guchhait, *Spectrochim. Acta Part A Mol. Biomol. Spectrosc.*, 2011, **78**, 1525–1534.

RSC Advances Accepted Manuscript

39 J. R. Lakowicz, Ed., *Principles of Fluorescence Spectroscopy*, Springer US, Boston, MA, 2006.

40 N. C. Maiti, M. M. G. Krishna, P. J. Britto and N. Periasamy, *J. Phys. Chem. B*, 1997, **101**, 11051–11060.

41 S. S. Mati, T. K. Mondal, S. Dhar, S. Chall and S. C. Bhattacharya, *Spectrochim. Acta - Part A Mol. Biomol. Spectrosc.*, 2012, **92**, 122–130.

42 A. Mallick, B. Haldar, S. Maiti and N. Chattopadhyay, *J. Colloid Interface Sci.*, 2004, **278**, 215–223.

43 M. Almgren, F. Grieser and J. K. Thomas, *J. Am. Chem. Soc.*, 1979, **101**, 279–291.

44 S. K. Ghosh, P. K. Khatua and S. C. Bhattacharya, *J. Colloid Interface Sci.*, 2004, **275**, 623–631.

45 H. Kumar, V. Devaraji, R. Joshi, M. Jadhao, P. Ahirkar, R. Prasath, P. Bhavana and S. K. Ghosh, *RSC Adv.*, 2015, **5**, 65496–65513.

46 X. Zhao, R. Liu, Z. Chi, Y. Teng and P. Qin, *J. Phys. Chem. B*, 2010, **114**, 5625–5631.

47 A. Maciejewski, D. R. Demmer, D. R. James, A. Safarzadeh-Amiri, R. E. Verrall and R. P. Steer, *J. Am. Chem. Soc.*, 1985, **107**, 2831–2837.

48 D. Bose, D. Sarkar, A. Girigoswami, A. Mahata, D. Ghosh and N. Chattopadhyay, *J. Chem. Phys.*, 2009, **131**, 114707.

RSC Advances Accepted Manuscript

49 G. A. Frisch, M. J.; Trucks, G. W.; Schlegel, H. B.; Scuseria, G. E.; Robb, M. A.; Cheeseman, J. R.; Scalmani, G.; Barone, V.; Mennucci, B.; Peterson , et al. Gaussian 09, Revision D.01; Gaussian, Inc.:Wallingford, CT 2009.

50 W. Kohn and L. J. Sham, *Phys. Rev.*, 1965, **140**, A1133–A1138.

RSC Advances Accepted Manuscript

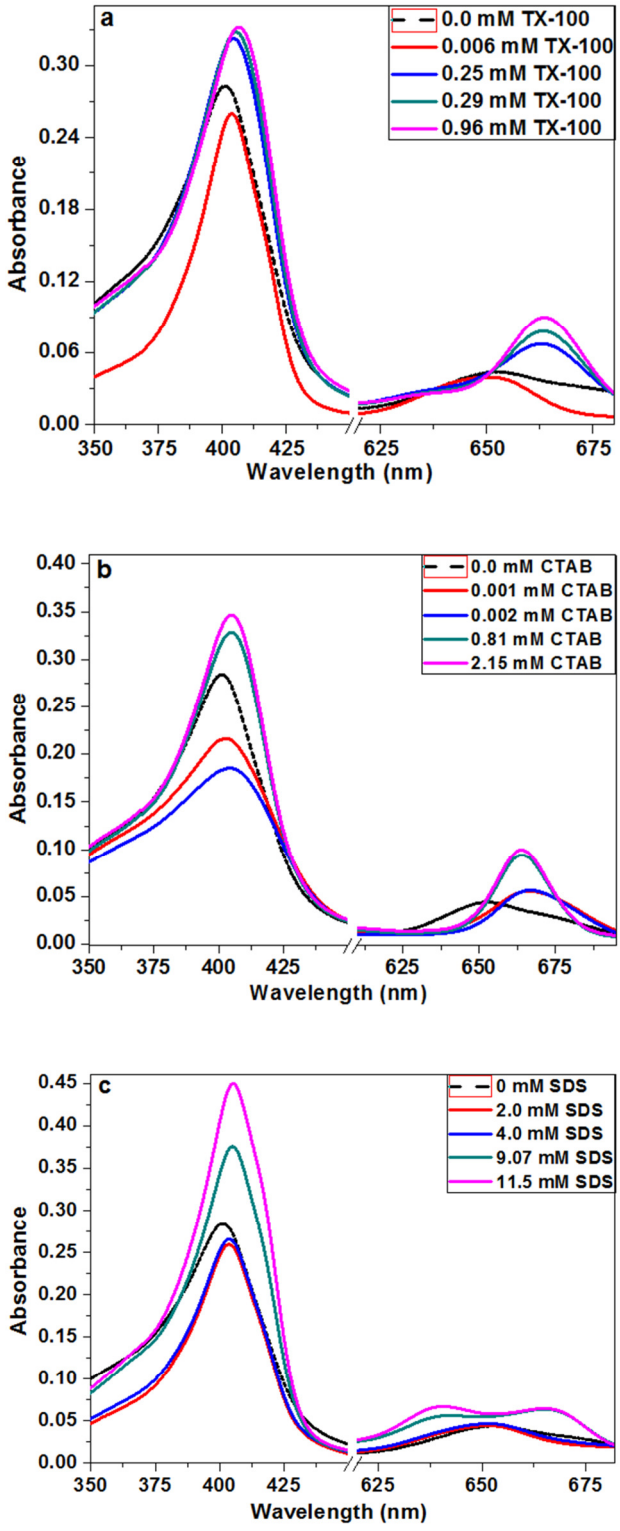

Figure 1: Absorption spectra of Chlorin e6 with increasing concentration of a) TX-100 b) CTAB and c) SDS at 298 K.

RSC Advances Accepted Manuscript

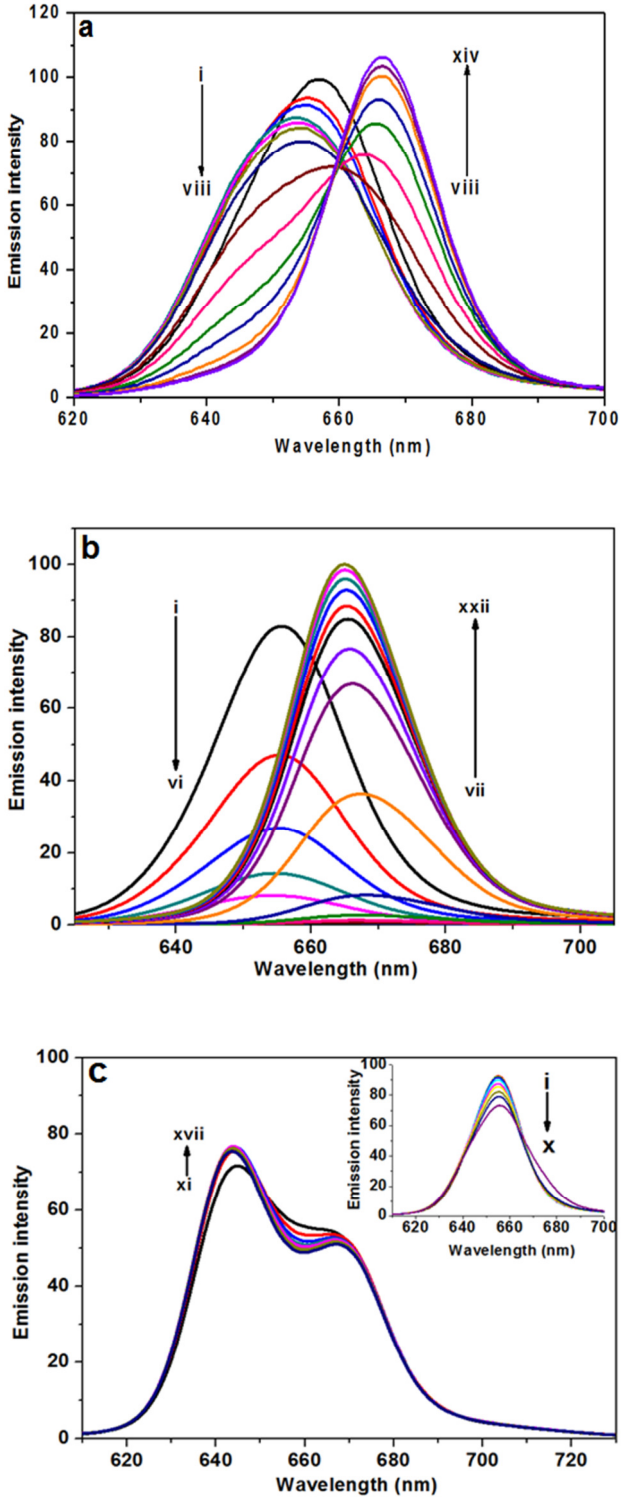

Figure 2: Emission spectra of Ce6 in aqueous medium at pH 7.4 at 298 K with increasing concentration of (a) TX-100 conc. (i to viii) 0.00, 0.005, 0.02, 0.04, 0.10, 0.15, 0.20, 0.23, (ix to

RSC Advances Accepted Manuscript

xiv) 0.27, 0.30, 0.40, 0.60, 0.80, 1.10 mM. (b) CTAB conc. (i to vi) 0, 0.001, 0.002, 0.003, 0.005, 0.02 (vii to xxii) 0.025, 0.05, 0.09, 0.30, 0.50, 0.60, 0.70, 0.80, 0.90, 1.00, 1.25, 1.50, 2.00, 3.00, 4.00 and 5.00 mM (c) Postmicellar conc. of SDS (xi to xvii) 8.0, 9.0, 10.0, 11.0, 12.0, 13.0, 14.0 mM, inset show premicellar change in emission spectra of Ce6 with increasing SDS conc. from (i to x) 0.0, 0.25, 0.50, 1.00, 2.00, 3.00, 4.00, 5.0, 5.50, 6.50.

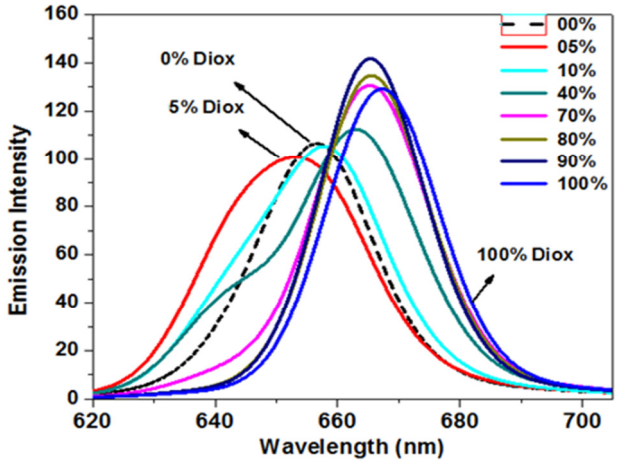

Figure 3: Emission spectra of Ce6in different water-dioxane mixture.

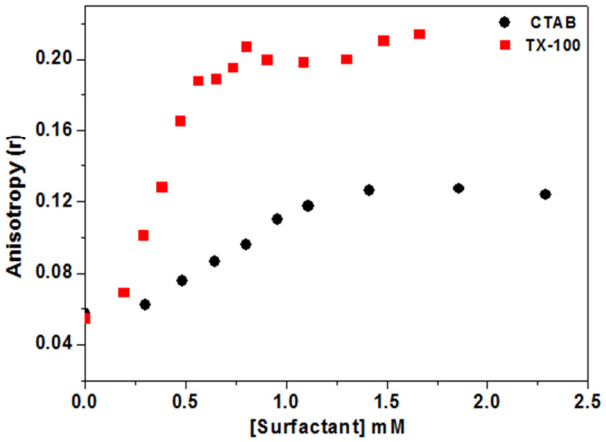

Figure 4: Plot of anisotropy value of Ce6 with increasing concentration of TX-100 and CTAB (λ_{ex} and λ_{em} are used as respective absorption and emission maxima).

RSC Advances Accepted Manuscript

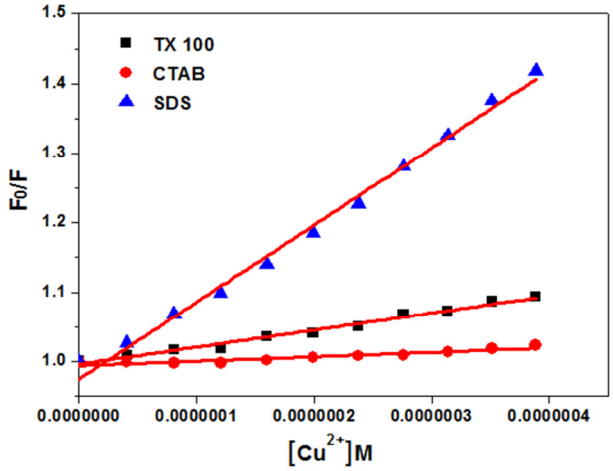

Figure 5: Plot of F_0/F versus $[Cu^{2+}]$ for the determination of quenching constant in different micellar medium.

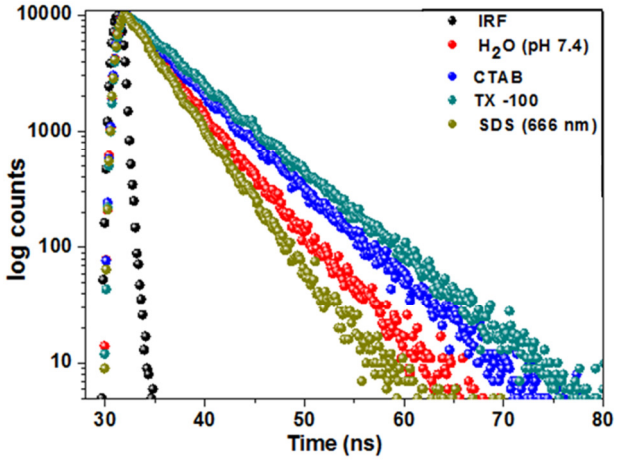

Figure 6: Fluorescence decay curve of Ce6 in different medium at room temperature.

RSC Advances Accepted Manuscript

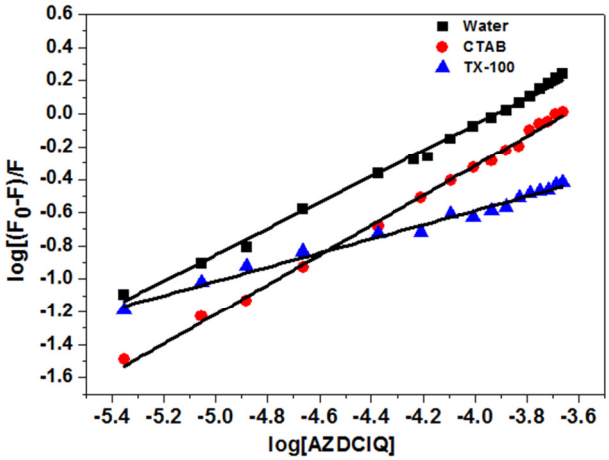

Figure 7: Determination of association constant (K_a) of Ce6 and AZDCIQ in water, CTAB, and TX-100.

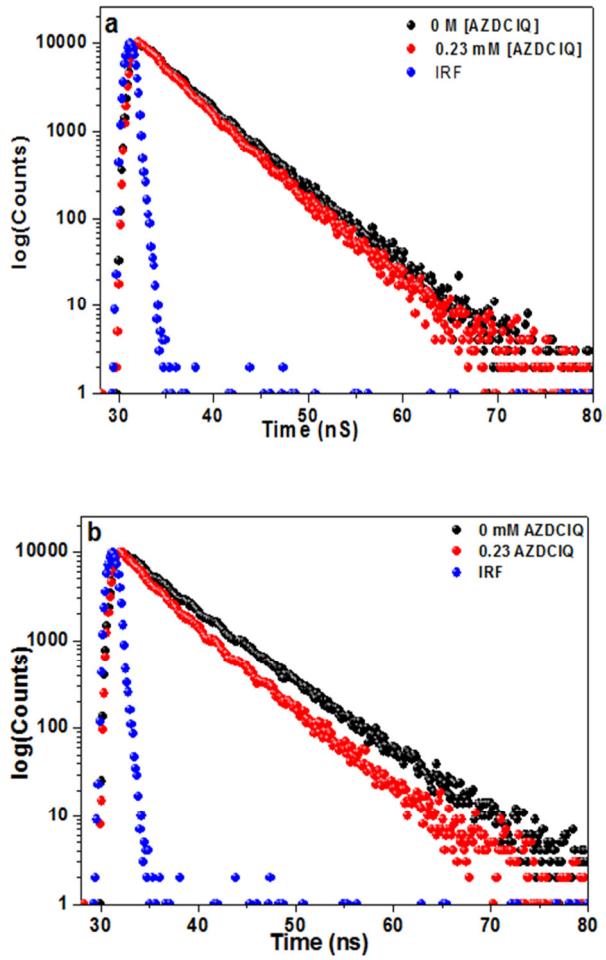

RSC Advances Accepted Manuscript

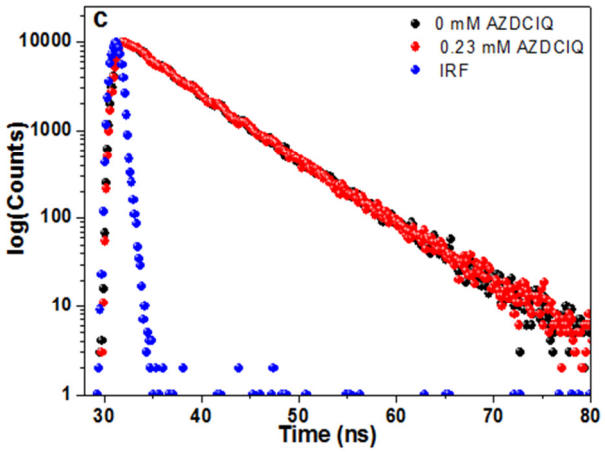

Figure 8: Fluorescence decay curve of Ce6 in the absence and presence of 2.3 x 10^{-4} M AZDCIQ in a) Water, b) CTAB and c) TX-100.

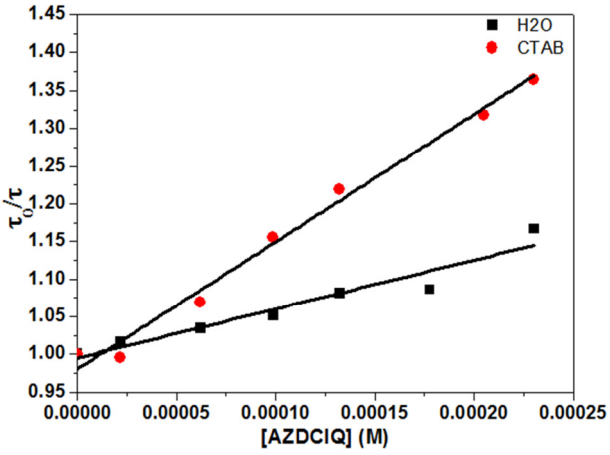

Figure 9: Stern-Volmer plot using average lifetimes obtained from biexponential fitting of the fluorescence decay curve of Ce6 in water and in fully micellized CTAB.

RSC Advances Accepted Manuscript